약학석사학위논문

The metabolic comparison between normal and lung cancer cell lines in the anoikis condition

아노이키스 (Anoikis) 환경에서
폐 정상세포와 폐암 세포의 대사양상비교

2018년 2월

서울대학교 대학원

약학과 천연물과학전공

추 문 기

The metabolic comparison between normal and lung cancer cell lines in the anoikis condition

아노이키스 (Anoikis) 환경에서

폐 정상세포와 폐암 세포의 대사양상비교

지도교수 박 성 혁

이 논문을 약학석사학위논문으로 제출함

2018년 2월

서울대학교 대학원
약학과 천연물과학전공
추 문 기

추 문 기의 석사학위논문을 인준함

2018년 2월

위 원 장 _____ (인)

부위원장 _____ (인)

위 원 _____ (인)

Abstract

The metabolic comparison between normal and lung cancer cell lines in the anoikis condition

CHOO MUN KI

Natural Products Science Major

College of Pharmacy

The Graduate School

Seoul National University

Lung cancer is a fatal disease with a low survival rate because it has little or no symptoms in the advanced stage. Further, it has the highest mortality, 22.6%, among all cancers in Korea. Generally, when normal cells lose their interaction with the matrix, it results in a phenomenon called anoikis as a defense mechanism of the living body, and the cells die. Tumors can be completely removed from the primary

site without metastasis; therefore, cancer cells can survive, and this plays an important role in the early stages of cancer metastasis. Therefore, by studying the anoikis resistance of cancer cells, we can prevent cancer metastasis and improve the existing cancer treatment methods. In this study, we compared the difference between the metabolism of normal and cancer cells; further, we analyzed how cancer cells can be resistant to anoikis. First, we compared the cell viability of the lung cancer cell (A549) and the normal cell (MRC5) in the anoikis condition, establishing time points of 8 h, the time point when the cell survival rate starts to change, and 29 h, the time point that shows the most different survival rate. Using metabolic analyses, the ratio of GSH (reduced)/total glutathione in the normal cells dipped notably at 29 h. This indicates that normal cells die because they cannot overcome the increased oxidative stress. Furthermore, the ^{13}C glucose flux data of the energy metabolites (e.g., ATP, CTP, etc.) using stable isotope labeling showed a significant reduction of M + 5 of energy metabolites, especially at 29 h in normal cells. The M + 5 labeling of ATP corresponded to the ribose ring with ^{13}C glucose labeled. In other words, it was possible to deduce that some specific step of purine synthesis was down regulated from glucose to ATP. De novo purine biosynthetic enzyme PPAT was decreased in the normal cells using real-time PCR. In terms of cancer, pyruvate carboxylase (PC) of the cancer was significantly increased at 29 h than at 8 h in the anoikis condition. Moreover, the total amount of NADPH was higher in the cancer cells, indicating that it was actively using the pentose phosphate pathway (PPP). Consequently, it contributed to the survival of cancer cells under the anoikis

condition. Studies have shown that metabolic differences between the normal and cancer cells might play an important role in anoikis resistance. This could provide a new perspective for future studies of metastasis and resistance to lung cancer.

Keywords: anoikis, anoikis resistance, lung cancer, metastasis, metabolomics

Student number: 2016-21857

Contents

List of Abbreviations

SIRM : Stable Isotope-Resolved Metabolomics

PC : Pyruvate Carboxylase

PPP : Pentose Phosphate Pathway

F6P : fructose 6-phosphate

Glc : glucose

Glc-6-P : glucose 6-phosphate

G3P : glyceraldehyde 3-phosphate

LAC : lactate

6PG : 6-phosphogluconate

PYR : pyruvate

R5P : ribose-5-phosphate

List of Figures

I. Introduction

Lung cancer is a fatal disease with a low survival rate because it presents few or no symptoms in the advanced stage.[1] Lung cancer is classified as Small Cell Lung Cancer (SCLC) and Non-Small Cell Lung Cancer (NSCLC), depending on the tissue type.[2] The reason for this distinction is that SCLS is unique from other types of lung cancers in terms of treatment and prognoses, thus biopsy is very important for determining the therapeutic decision. NSCLC accounts for about 85% of all lung cancers and is relatively less sensitive to chemotherapy compared to SCLC. The most common types of NSCLCs are squamous cell carcinoma, large cell carcinoma, and adenocarcinoma.[3] Squamous cell carcinoma is mostly associated with cigarette smoking and has relatively slower proliferation; however, it is well metastasized in the liver, adrenal gland, central nervous system, and pancreas.[4]

According to the data released by the Health Insurance Review & Assessment Service (HIRA), lung cancer has the highest mortality, 22.6%, among all cancers in Korea. The 5-year survival rate of lung cancer was about 25% in 2015, lower than that for other cancers. Moreover, 85% of lung cancer cases are already metastasized when diagnosed, and the 5-year survival rate for metastatic lung cancer is only 4%. Thus, lung cancer metastasis is a crucial aspect.

There is a correlation between cancer metastasis and anoikis.[5] Anoikis is a kind of programmed cell death that occurs when anchorage-dependent cells detach from the

extracellular matrix (ECM).[6] The ECM provides an essential signal for cell growth or survival[7], and when detached from the ECM, normal cell-matrix interaction decreases, leading to anoikis.[8, 9]

Generally, when normal cells lose their interaction with the matrix, it causes a phenomenon called anoikis as a defense mechanism of the living body resulting in cell death. By contrast, cancer cells can survive in the same situation, and this plays an important role in the early stages of cancer metastasis.[10] Therefore, by studying the anoikis resistance of cancer cells, we may have a clue to prevent cancer metastasis and improve the existing cancer treatment methods.[11, 12] In order to study the metabolism in the anoikis condition, we used a stable isotope analysis technique.[13, 14] Previous methods engaged in biology have focused on measuring the transcript, enzyme and metabolite concentrations. These may be suitable for discriminating control and disease; however, they could not provide practical information about alterations in the metabolic pathway.

Therefore, a broadly accessible system for quantitative studies of the metabolomics is essential. The Stable Isotope-Resolved Metabolomics (SIRM) is useful for mapping the flow of carbon across the total biochemical network.[15] SIRM is performed by supplying the cells with an isotope labeled substrate (e.g., ^{13}C-labeled glucose or glutamine) and measuring the isotope transfer pattern that appears in the downstream metabolite using a mass spectrometer (MS) or with nuclear magnetic resonance (NMR).[16],[17] For example, the metabolites produced by the pathway can yield different mass changes affecting the mass isotopomers distribution (MID) of

the final product that can be measured using MS analysis. The patterns of MID can be analyzed to identify the metabolic pathways that are activated or down regulated.

In this project, we studied how cancer cells acquire the resistance to anoikis by comparing and analyzing the metabolisms after anoikis induction in normal and cancer cells. This may provide a new perspective for future studies on lung cancer metastases and resistance to lung cancer.

II. Materials and Methods

1. Cell Culture

Human lung adenocarcinoma A549 and human lung fibroblast MRC5 were purchased from Korean Cell Line Bank (KCBL, Seoul, Korea) and maintained in high-glucose(25mM) Dulbecco's modified Eagle's medium (DMEM, Welgene, Gyeongsan-si, Korea). All culture media were supplemented with 10% fetal bovine serum (FBS, Welgene, Gyeongsan-si, Korea), 1% penicillin/streptomycin (Gibco, NY, USA) and incubated at 37°C under 5% of CO_2 humidified air. For stable isotope labeling, 5.5 mM of [U-^{13}C] glucose (CLM-1396-5, Cambridge Isotope Laboratories, MA, U.S.A.) was added to cell culture medium, and the cells were incubated at 37℃.

2. Poly-HEMA coating plate for anoikis condition

To make low adhesion dishes, 6 well plates (H31106, Hyundai micro, Seoul, Korea) were coated with Poly-HEMA (Poly 2-hydroxyethyl methacrylate; P3932, Sigma, MO, USA). 0.5g of Poly-HEMA was dissolved in 1000ml 95% EtOH by sonicating several hours. This gives a 0.5 mg/ml solution. 6 well plates were coated with 6ml/well and dry overnight at 45℃, 3 times. Plates were wrapped in bags and stored indefinitely at 4℃ prior to use.

3. Cell sample preparation for LC-MS

The metabolites were extracted using two phase methanol-chloroform extraction methods. Cell pellets were re-suspended with the mixture of 400 μL methanol and 200 μL chloroform. Three cycles of the following steps were then repeated: dipping into liquid nitrogen for 1 min, thawing at room temperature for 2 min. After additionally adding a mixture of 200 μL chloroform and 200 μL distilled water, the samples were centrifuged at 15,000 g for 20 min at 4℃. The upper water phase and lower lipid phase were collected and dried with a centrifugal vacuum evaporator (Vision, Seoul, Korea). The middle phase, proteins, were collect for the normalization. 1M urea was added to proteins to denature and shaken overnight, and quantified using a BCA Protein Assay Kit (Pierce, Appleton, WI). The upper phase pellets were dissolved in 20 μL mixture of HPLC-grade acetonitrile and water (1:1, v/v) for LC-MS.

4. Metabolite analysis by LC-MS

For LC-MS analysis, the extracted metabolites were injected with an injection volume of 5 μL. HPLC was performed on an Agilent 1100 Series liquid chromatography system equipped with a degasser, an auto-sampler, and a binary pump (Agilent, Santa Clara, CA, U.S.A.). Sample separation was achieved by a ZIC-pHILIC Polymeric Beads Peek Column (150 × 2.1 mm, 5 μm, Merck kGaA, Darmstadt, Germany) at 35°C, and the temperature of auto-sampler was set at 4°C.

For the solvent system, mobile phase A and B were distilled water with 10 mM ammonium carbonate (pH = 9.1) and acetonitrile. The mobile phase was delivered at a flow-rate of 0.15 mL/min and the entire eluent was carried into a mass spectrometer. The linear gradient was as follows: 80% B at 0 min, 35% B at 10 min, 5% B at 12 min, 5% B at 25 min, 80% B at 25.1 min, and 80% B at 35 min. Mass spectra were obtained in negative and positive ion mode using an LTQ Mass Spectrometer (Thermo, USA).

5. Reverse transcriptase-polymerase chain reaction (RT-PCR) and Real-time Polymerase chain reaction (qPCR)

Total RNA was isolated from cell lines by easy-spin^{TM} Total RNA Extraction Kit (Intron, Seoul, Korea). The cDNA was synthesized by High Capacity cDNA Reverse Transcription Kit (Applied Biosystem, U.S.A.) following the manufacturer's instruction. Real-time PCR reaction was performed in triplicate in an Applied Biosystems 7300 PCR machine with SYBR green –based detection (iTaq TM Universal SYBR Green Supermix, Cat. No. 172-5120, Bio-Rad, USA). The gene expression ΔCt value of PC was calculated by normalization with b-actin.

The primer sequences of PC, b-actin as follows :

PC sense : 5'-GCAAGATGGGAGACAAGGTG-3'

PC antisense : 5'-AGTAGGCCCGGGTGTAATTC-3'

b-actin sense : 5'-GGACTTCGAGCAAGAGATGG-3'

b-actin antisense : 5'-AGCACTGTGTTGGCGTACAG-3'

6. Western blot

For Western blot analysis, cells grown in the anoikis condition were harvested at 8 h and 29 h. For protein extraction, cells were suspended in 100 ul of RIPA buffer containing protease inhibitors (1 μg/ml of Aprotinin, 1 μg/ml of Pepstatin, and 2 μg/ml of PMSF) and phosphatase inhibitors (4 μg/ml of Sodium Fluoride and 25 μg/ml Sodium Orthovanadate) and put on ice for 30 min. The supernatant containing the total protein from the cell was harvested after centrifugation twice at 10,000 g for 10 min, and quantified using a BCA Protein Assay Kit (Pierce, Appleton, WI). 30mg of total protein was subjected to 10% SDS-PAGE, and the resolved proteins were transferred to nitrocellulose membranes (Bio-Rad). The membrane was blocked with 5% skim-milk and blotted with antibodies against PC (PCB (C-13) Antibody Santa SC-46228 goat polyclonal) - 1:1000 in TBST and as a loading control, β-actin(Antibody Santa SC-47778 mouse monoclonal) - 1:1000 in TBST

was used at 4°C overnight and followed by incubation secondary antibody - rabbit anti-goat IgG-HRP (Santa SC-2922) in 1:10000 in 2.5% skim milk TBST and goat anti-mouse IgG (Abfrontier LF-SA8001) 1:10000 in TBST at Room temperature for 1h. The protein bands were visualized using the enhanced chemiluminescence (ECL) detection kit EZ-Western (DOGEN, DG-W250, Seoul, Korea). Blots were analyzed by LAS4000 (GE Healthcare, ImageQuant)

III. Results

1. Cell viability and proliferation assay in the anoikis condition

First, when studying the effects of anoikis on cell metabolism, the viability of cells was an important consideration. We compared the cell viability of the lung cancer cell line (A549) and the normal cell line (MRC5) using MTT assay in the anoikis (Fig. 1A). After setting the time condition, we confirmed the proliferation by counting (Fig. 1B). In the anoikis condition, cancer cells grew; however, the normal cells decreased.

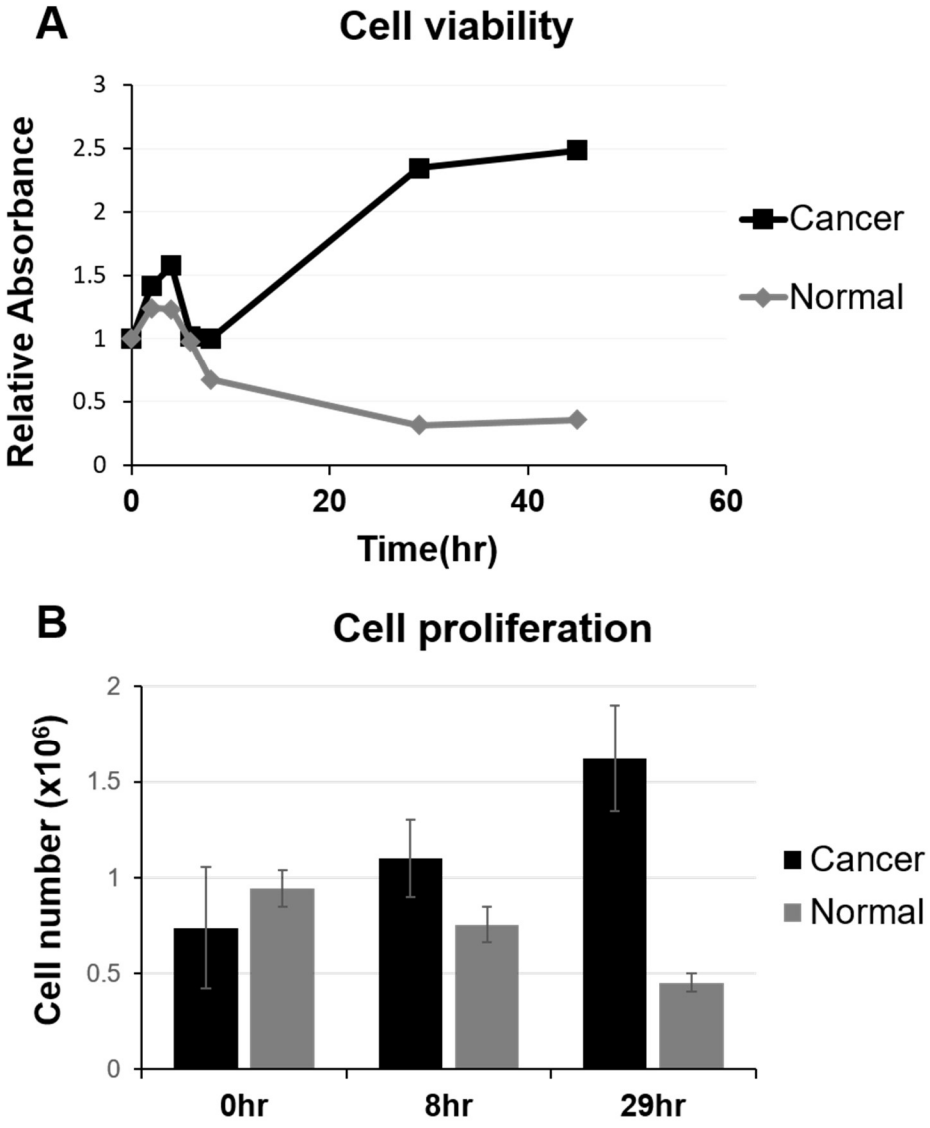

Figure 1. Cell Viability and Proliferation Assay

(A) MTT assay, In the anoikis condition, the viability of MRC5 and A549 cells was analyzed by MTT assay. We established time points 8 h the time point when the cell survival rate starts to change, and 29 h, the time point with the most different survival rate. **(B)** Identifying the proliferation by cell counting.

2. Overall metabolite analysis

We checked the ^{13}C-labeling pattern of some metabolites to identify the ones that were different between the cancer and normal cells. The alterations of malate and NADPH were distinct in the cancer cells; by contrast, the changes in GSH, GSSG, and ATP were noticeable in the normal cells (Fig 2).

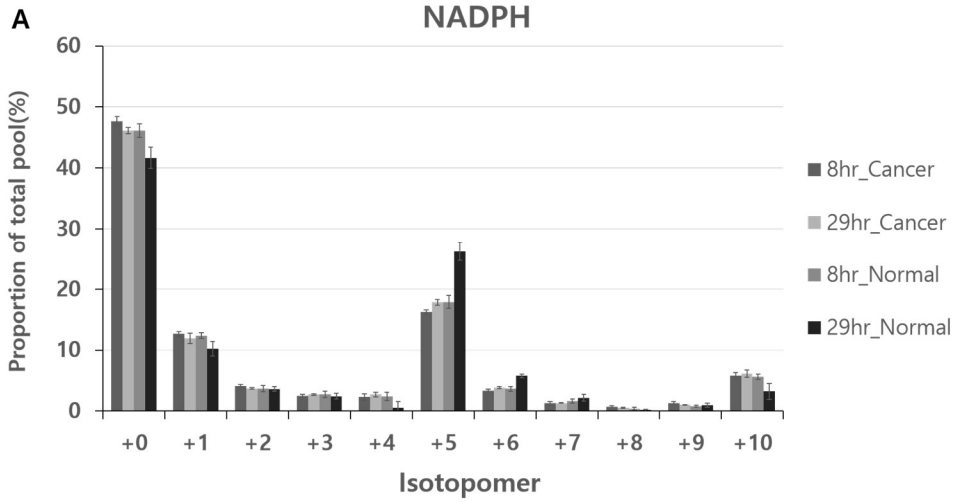
A
NADPH
Proportion of total pool(%)
60
50
40
30
20
10
0
+0
+1
+2
+3
+4
+5
+6
+7
+8
+9
+10
Isotopomer
8hr_Cancer
29hr_Cancer
8hr_Normal
29hr_Normal

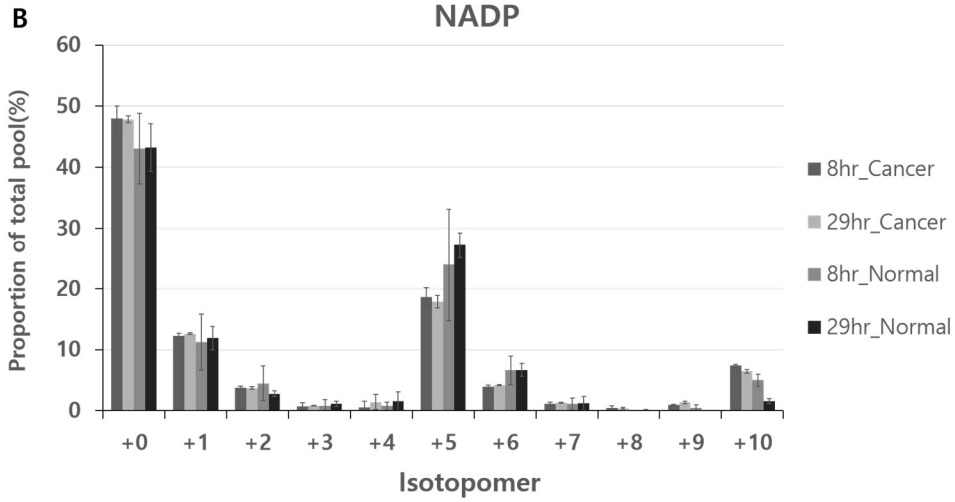
B
NADP
Proportion of total pool(%)
60
50
40
30
20
10
0
+0
+1
+2
+3
+4
+5
+6
+7
+8
+9
+10
Isotopomer
8hr_Cancer
29hr_Cancer
8hr_Normal
29hr_Normal

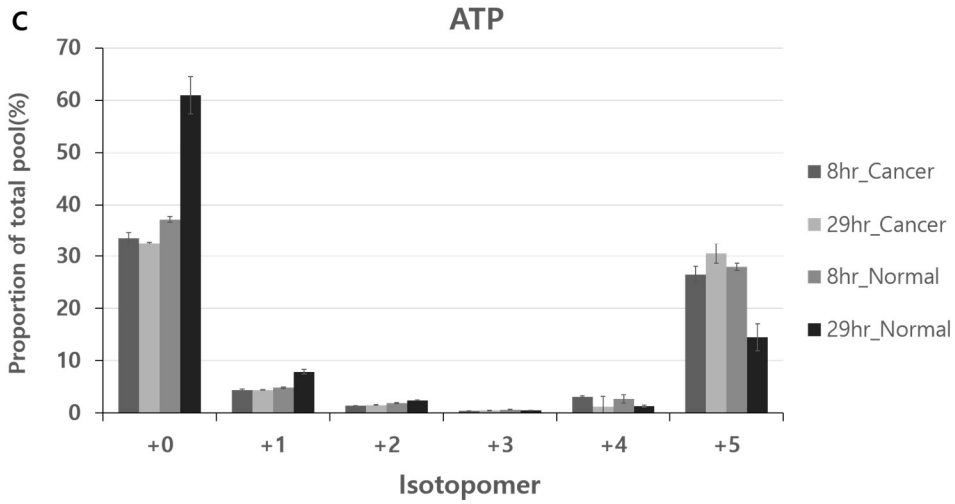
C
ATP
Proportion of total pool(%)
70
60
50
40
30
20
10
0
+0
+1
+2
+3
+4
+5
Isotopomer
8hr_Cancer
29hr_Cancer
8hr_Normal
29hr_Normal

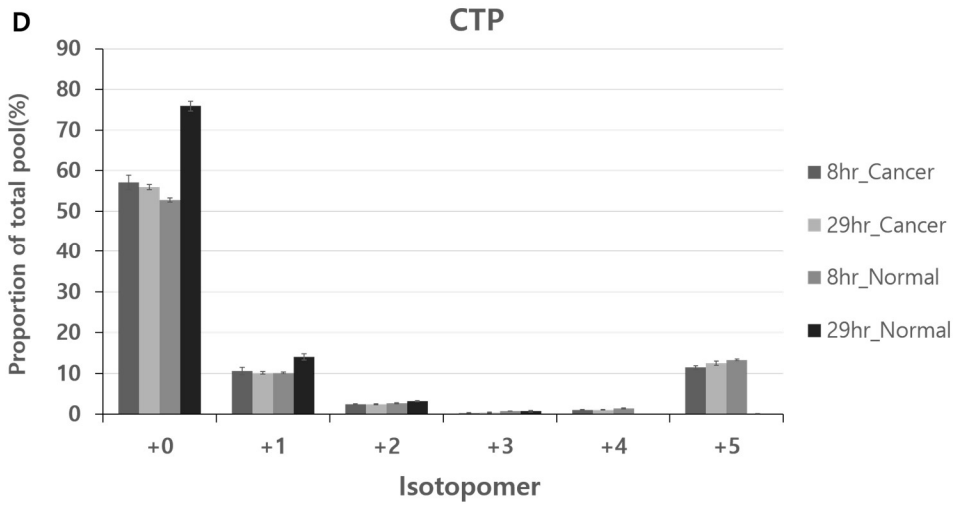
D
CTP
Proportion of total pool(%)
90
80
70
60
50
40
30
20
10
0
+0
+1
+2
+3
+4
+5
Isotopomer
8hr_Cancer
29hr_Cancer
8hr_Normal
29hr_Normal

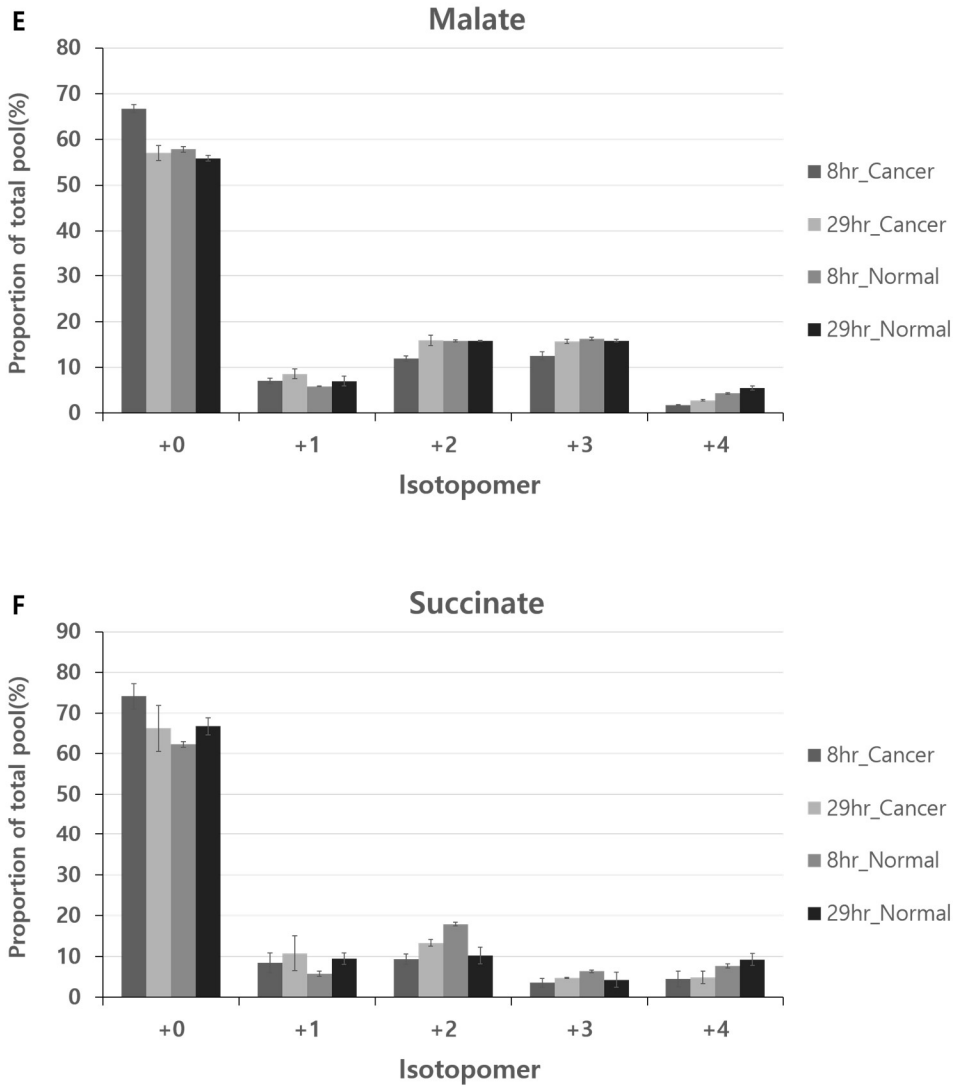

Figure 2. ^{13}C-labeling pattern of metabolites

(A) NADPH, (B) NADP, (C) ATP. (D) CTP, (E) Malate, (F) Succinate

The bar charts represent labeling patterns of some metabolites in cancer and normal.

3. Pyruvate carboxylase (PC) increased in the cancer cells at 29 h, as inferred from $^{13}C_3$-malate

In addition, there were significant changes in $^{13}C_3$-malate in cancer cells. In contrast, the change in the $^{13}C_3$-malate was relatively consistent in the normal cells (Fig. 3). The increment in $^{13}C_3$-malate is thought to be due to an increased PC activity.

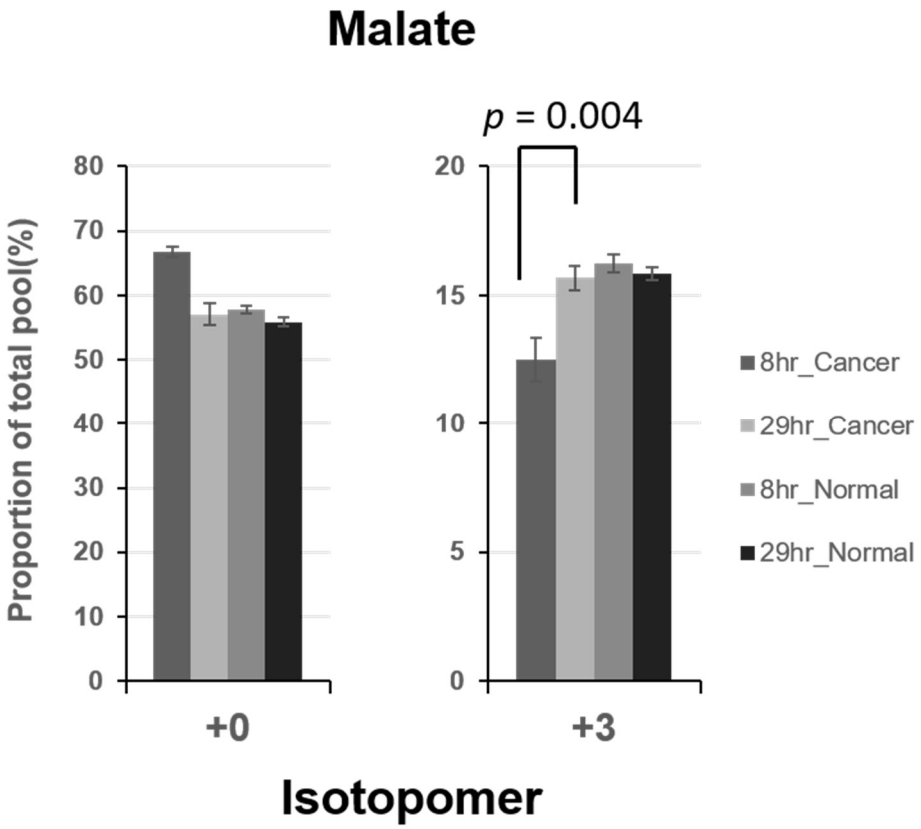

Figure 3. ^{13}C labeling pattern of Malate

The bar chart represents the relative labeling patterns of malate in cancer and normal. There was an important alteration in $^{13}C_3$-malate in cancer cells.

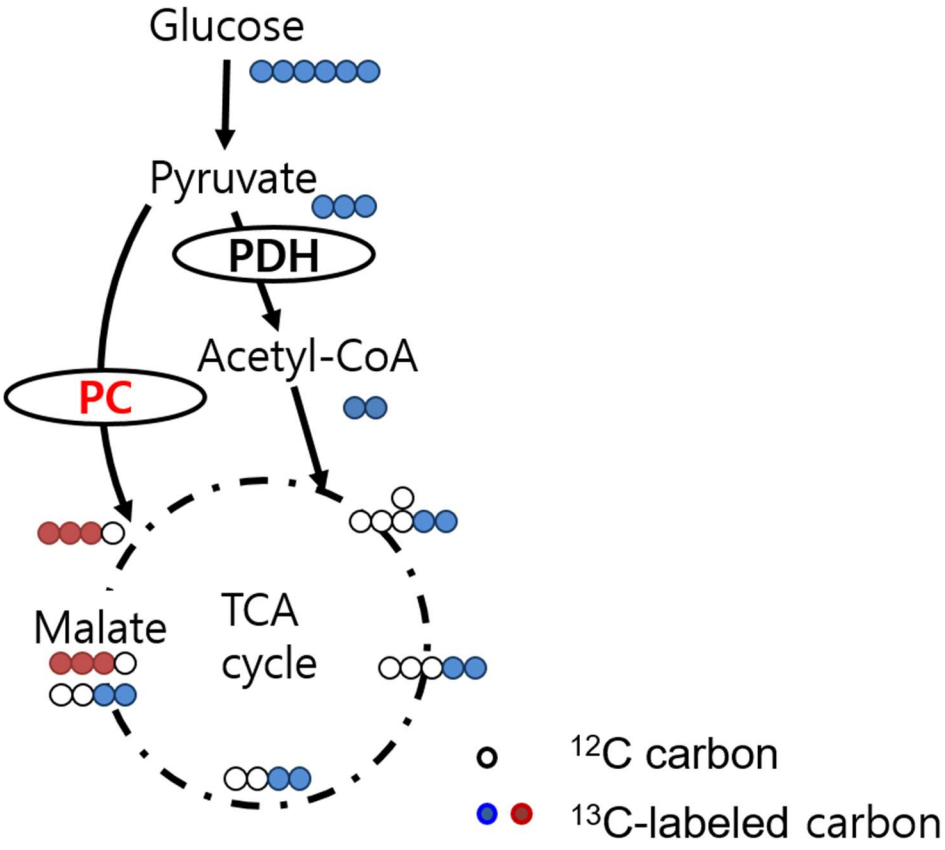

Figure 4. An atom-resolved map illustrates how PC produces the ^{13}C isotopologs of malate

PC and PDH catalyze the major inputs into the Krebs cycle to support the anabolic demand for biosynthesis. Also shown is the fate of ^{13}C from $^{13}C_6$-glucose through glycolysis and into the Krebs cycle via PC (red) and PDH (blue).

In figure 4, full labeling of $^{13}C_6$-glucose passes through the PC and produces three labeled $^{13}C_3$-malate.[18] Therefore, it was assumed that the PC activity was increased in cancer, giving resistance to the anoikis condition. Consequently, Western blot analysis was conducted to confirm the amount of PC.

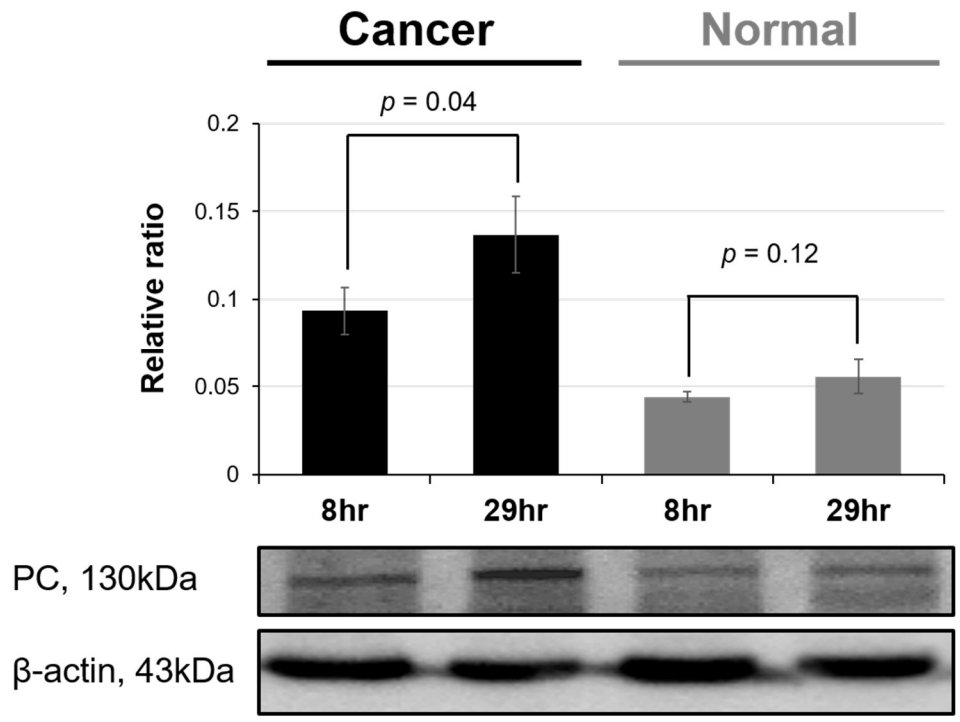

Figure 5. Representative Western blots of PC protein expression levels in cancer and normal cell lines

The protein expression measured by western blot assay. The protein extract of the anoikis condition at 8 h and 29 h were obtained. The expression of PC was detected in cancer and normal. The graph of relative ratio shows representative of the results acquired from three independent experiments.

At the protein level, the longer the exposure time in the anoikis condition, the more noticeable the increment in PC was confirmed in cancer cells (Fig. 5). This confirms that there is a correlation between the activity and amounts of PC, verifying that increase in PC results in anoikis resistance in cancer cells.

4. High levels of total NADPH from PPP in cancer cells

The total amount of NADPH was also high in cancer cells (Fig. 6). NADPH was produced mainly from Pentose phosphate pathway (PPP) (Fig. 7).

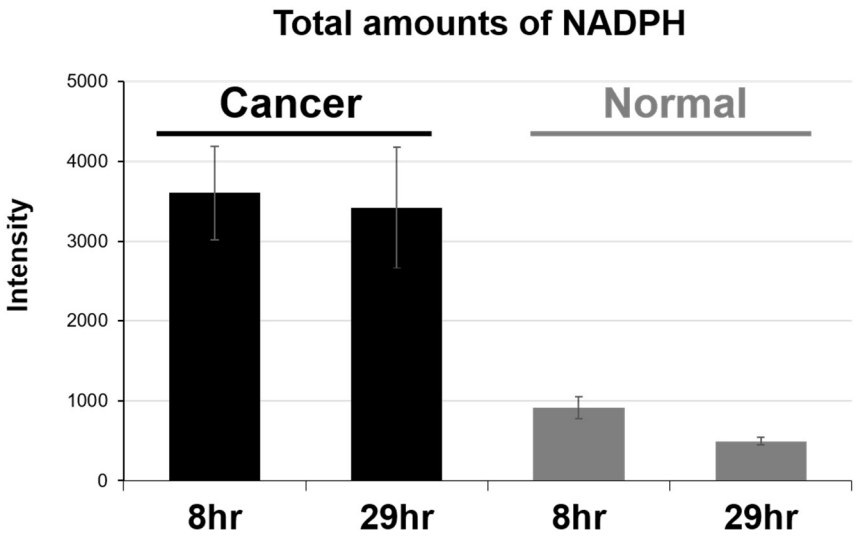

Figure 6. Bar chart of total amounts of NADPH in cancer and normal

The bar chart represents the intensity of NADPH in cancer and normal. There was a big difference between cancer and normal.

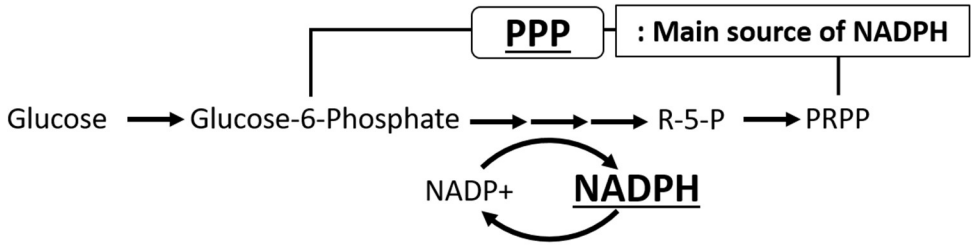

Figure 7. A plot of the relationship between NADPH and PPP

By measuring the carbon NMR using [1,2-$^{13}C_2$] glucose labeling, difference in the singlet and doublet peaks of lactate was used to determine whether PPP or glycolysis was dominant in the cell line. If PPP is dominant, the singlet peak will increase. If glycolysis is dominant, doublet peak will increase (Fig. 8).[19] Based on this, we applied it to our experiments and found that the singlet to doublet ratio in cancer cells was higher than that in the normal cells, indicating that cancer cells use PPP more actively (Fig. 9). Consequently, PPP activation contributed to the survival of cancer cells under the anoikis condition.

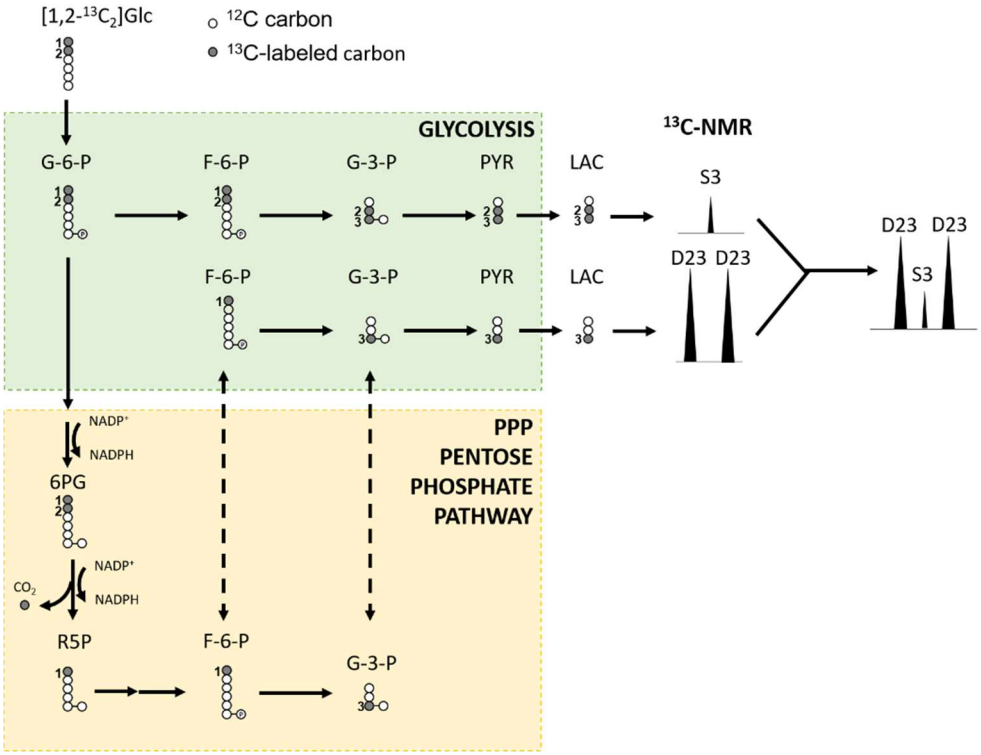

Figure 8. A plot of [1,2-$^{13}C_2$] glucose metabolism through glycolysis and PPP

The plot indicates that the resulting labeling pattern of lactate C3 by [1,2-$^{13}C_2$] glucose metabolism through glycolysis and PPP.

F6P, fructose 6-phosphate; Glc, glucose; Glc-6-P, glucose 6-phosphate; G3P, glyceraldehyde 3-phosphate; LAC, lactate; 6PG, 6-phosphogluconate; PYR, pyruvate; R5P, ribose-5-phosphate

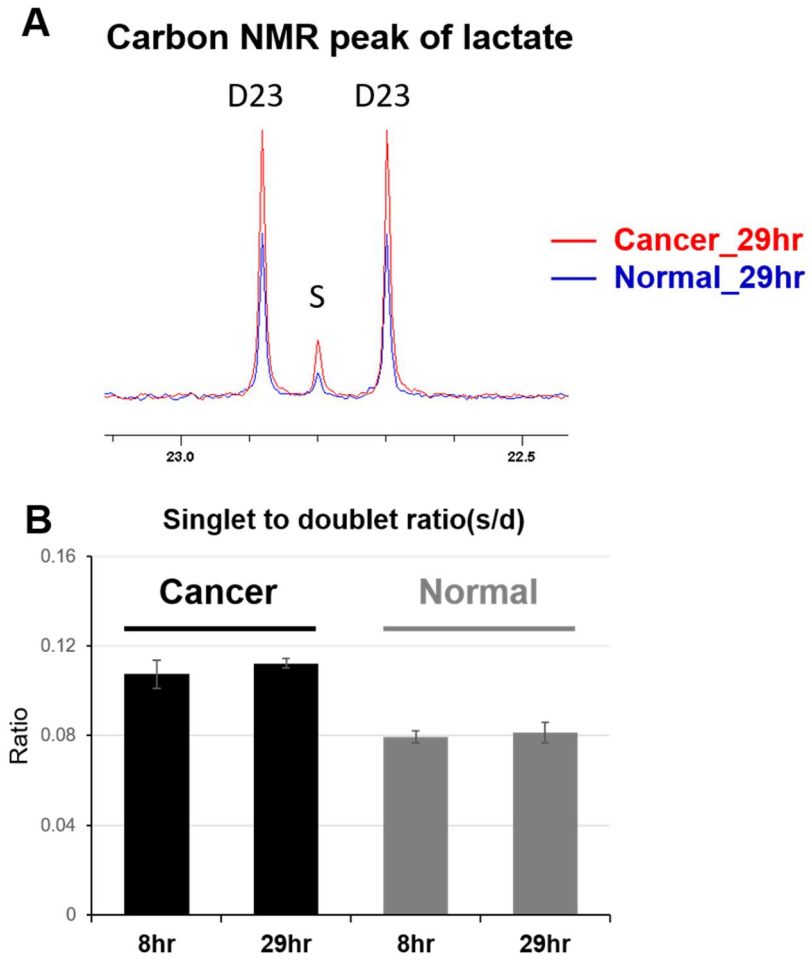

Figure 9. Peak ratio of lactate

(A) ^{13}C NMR spectrum illustrating the labeling pattern of lactate

As a consequence of the higher activity of relative PPP to glycolysis in cancer, the contribution of the singlet (S3) to doublet (D23) is significantly important.

(B) Singlet to doublet ratio of lactate in cancer and normal

The bar chart represents the ratio of s/d in cancer and normal. Cancer has high s/d ratio that indicates use PPP more actively

5. Oxidative stress is increased in normal cell lines at 29 h

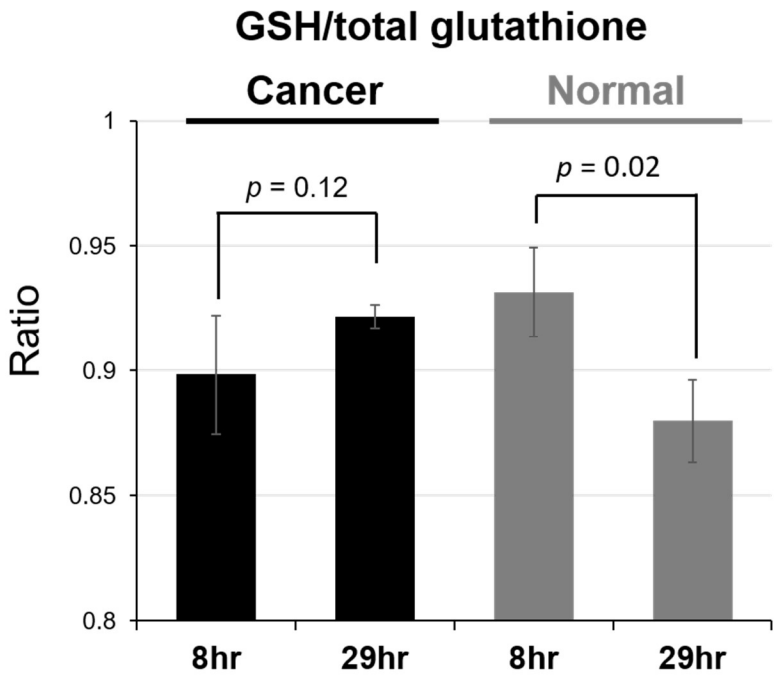

Figure 10. GSH/total glutathione ratio in cancer and normal

The bar chart represents the ratio of GSH/total glutathione in cancer and normal. In the normal cells, the ratio was decreased at 29 h. It means that the oxidative stress was greater than before.

The ratio of GSH (reduced)/total glutathione in the normal cells dipped notably at 29 h (Fig. 10), indicating that the oxidative stress was increased, which in turn suggests that normal cells die because they cannot overcome the increased oxidative stress.

6. ATP M+5 is decreased in normal cell line at 29 h

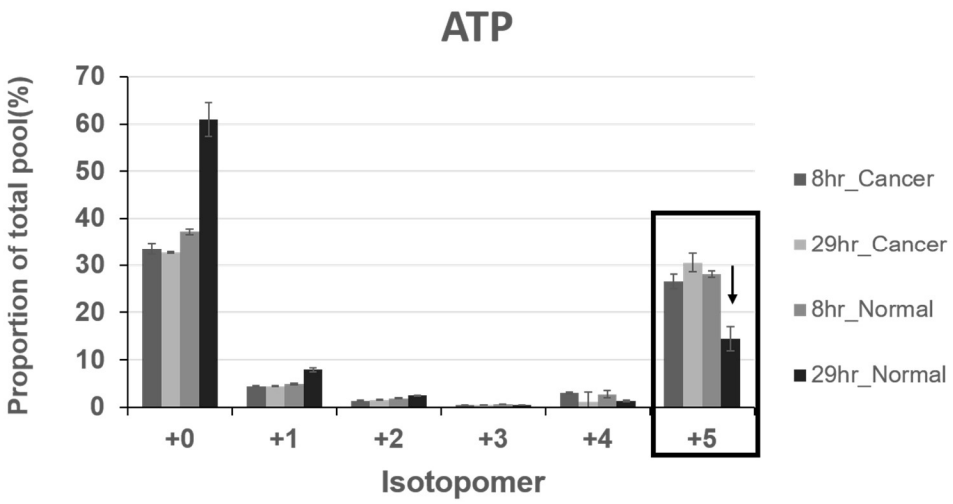

Figure 11. ^{13}C-labeling pattern of ATP

The bar charts represent labeling patterns of ATP in cancer and normal. There is an important decrease in M + 5 of ATP, especially at 29 h in the normal cells

The ^{13}C glucose flux data of the energy metabolite (e.g., ATP, CTP, etc.) using stable isotope labeling also showed a significant reduction in M + 5 of energy metabolites, especially at 29 h in the normal cells (Fig. 11). The M + 5 labeling of ATP corresponded to the ribose ring (Fig. 12A, circled area) that comes from ^{13}C glucose (Fig. 12B). In other words, it was possible to deduce that some specific step of purine synthesis was down regulated from glucose to ATP.

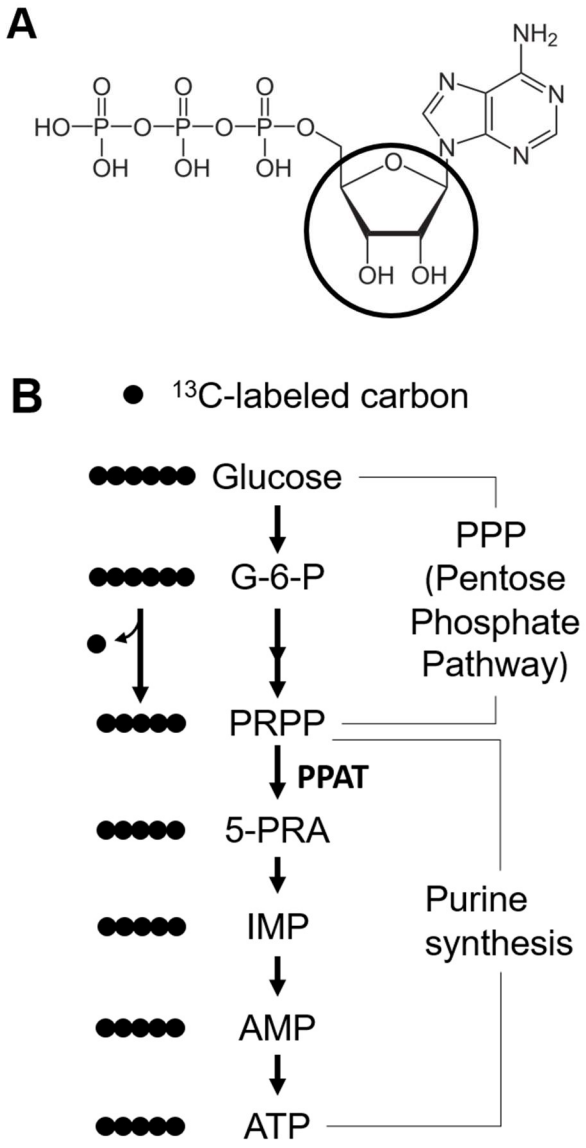

Figure 12. (A) Structure of ATP and (B) A synthesis scheme of ATP

Previously, in the experiment with 1,2-13C-glucose labeling, there was no significant difference in the PPP in the normal cells (Fig. 9B). Therefore, it seemed that the process after PPP is down-regulated. PPAT is an enzyme responsible for catalyzing the PRPP in de novo purine synthesis (Fig. 13). De novo purine biosynthetic enzyme PPAT was decreased in the normal cells, as measured using real-time PCR (Fig. 14). It was thought that the relative decrease in normal cells compared to that in the cancer cells would contribute to the death of normal cells in the anoikis condition.

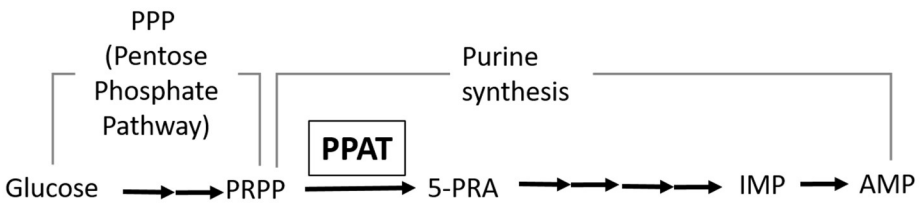

Figure 13. A plot of the purine synthesis

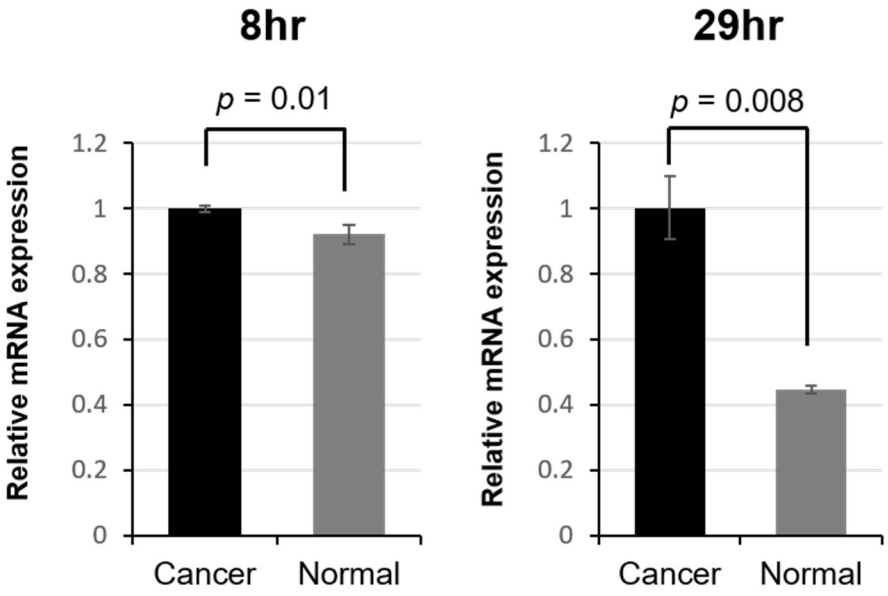

Figure 14. Bar chart of PPAT's real-time PCR

The bar chart represents the relative mRNA expression of cancer and normal in the anoikis condition at 8 h and 29 h analyzed by real-time PCR. De novo purine biosynthetic enzyme PPAT was decreased in the normal at 29 h.

IV. Discussion

Accumulating evidence suggests that anoikis resistance may play an important role in cancer metastasis.[5] When normal cells lose the interaction with ECM, it can induce anoikis as a defense mechanism. However, cancer cells can survive in the anoikis condition, a crucial step in cancer metastasis.[10] In particular the metabolic comparison between cancer and normal lung cancer cell lines in the anoikis condition has not been fully understood. Changed metabolisms in normal and cancer cell lines in the anoikis condition can provide valuable information for cancer metastasis in clinical practice. In this study, we examined the metabolic changes in response to anoikis in normal and cancer cell lines by metabolomics.

Results from the SIRM showed metabolic alterations of the cancer and normal cell lines. PC was increased in the cancer cells at 29 h of the anoikis condition, as inferred from $^{13}C_3$-malate. PC is an enzyme that catalyzes pyruvate to oxaloacetate (OAA).[20] This reaction is a crucial anaplerotic reaction that makes oxaloacetate from pyruvate. PC is an important factor in the gluconeogenesis, lipogenesis, and synthesis of neurotransmitters. Oxaloacetate produced from PC is an important intermediate used for several biochemical pathways.[21, 22] It has been established that PC is high in lung cancer tissue.[18] In the anoikis condition, the longer the exposure time, the more noticeable the increment of PC, as was confirmed using Western blot analysis.

Cancer cells were able to resist the anoikis condition by increasing their PC amount.

An increasing trend in the total amount of NADPH was seen in the cancer cells than in the normal cells.[23] Nicotinamide Adenine Dinucleotide Phosphate (NADP) is a major coenzyme present in living organisms along with nicotinamide adenine dinucleotide (NAD). NADPH, a reduced form of NADP, is an important reducing agent in vivo. NADP+/NADPH pairs provide redox potential in organisms.[24] NADPH allows GSH regeneration by providing a reducing equivalent for oxidation-reduction that protects against the biosynthesis reactions and toxicity of reactive oxygen species (ROS).[25] The PPP generates NADPH, a reducing agent used in reductive biosynthesis reactions. In this process, the cancer cells obtain NADPH and remove ROS to overcome the oxidative stress and enhance survival.[26] As can be seen in Fig 9, cancer cells can use PPP actively, consequently contributing to their survival under the anoikis condition.

In contrast, normal cells died as they could not overcome the increased oxidative stress. The ratio of GSH (reduced)/total glutathione in the normal cells dipped notably at 29 h. ROS are involved in multiple pathologies, including malignant diseases, chronic inflammatory process, ischemia, type II diabetes, atherosclerosis, and several neurodegenerative diseases. Further, ROS are essential in cell metabolism because they activate certain transcriptional factors and several enzyme cascades. Oxidative stress is a favorable unevenness to produce ROS through antioxidant barricades.[27]

Moreover, the amount of ROS in normal cells in the anoikis condition is increased,

and antioxidant treatment allows fatty acid oxidation and restoration of the low ATP levels in the normal breast cell line.[28, 29] . In the ^{13}C glucose flux data using stable isotope labeling, energy metabolites (e.g., ATP, CTP, etc.) showed a significant decrease in the M + 5 of energy metabolites, especially at 29 h in the normal cells. It is inferred that ATP could not be synthesized well; therefore, the normal cells were unable to survive in the anoikis condition. The M + 5 labeling of ATP is related to the ribose ring that comes from ^{13}C glucose. In other words, it was possible to deduce that some specific step of purine synthesis was down regulated from glucose to ATP. De novo purine biosynthetic enzyme PPAT was decreased in the normal cells, as measured using real-time PCR.

In summary, there are altered pathways in the anoikis condition (Fig. 15). The change in the oxidative stress related metabolites, NADPH, GSH, and GSSG as well as the energy related metabolite, ATP, was noticeable under the anoikis condition. Studies have shown that metabolic differences in normal and cancer cells might play an important role in anoikis resistance. Especially pyruvate carboxylase (PC) of lung cancer was dramatically increased in the anoikis condition, as treating with specific inhibitors for PC or siRNA could be a new therapeutic target for the lung cancer. Also in this project, we just used only one cancer cell line, but we can apply this metabolomic approaches to the other metastatic lung cancer cell lines. It could provide a new perspective for future studies of metastases and resistance to lung cancer.

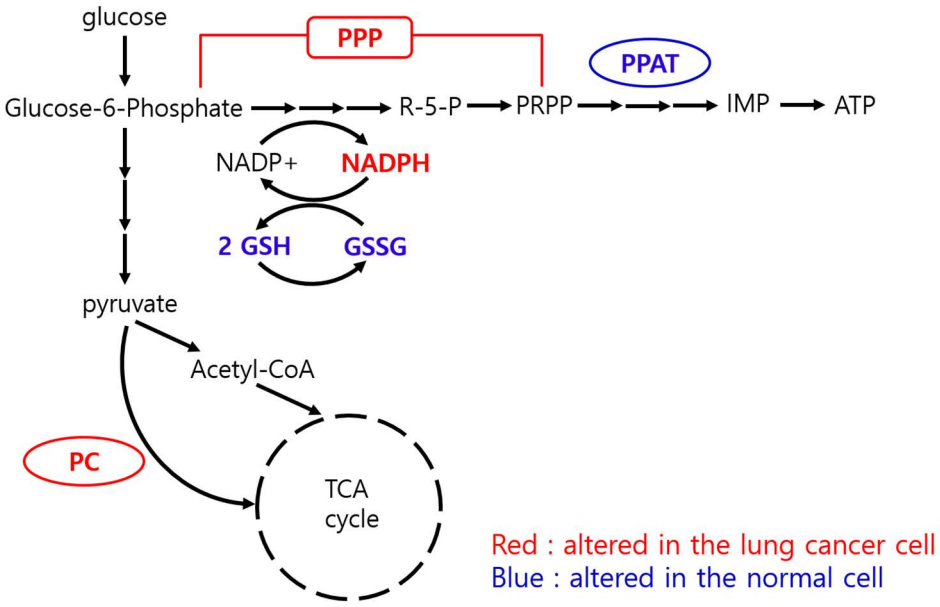

Figure 15. The altered pathway in the anoikis condition

V. References

1. Hong WK, Tsao AS. Lung carcinoma: Tumots of the lungs. merck manual professional edition. Online. 2007.

2. Mustafa M, JamalulAzizi A, IIIzam E, Nazirah A, AM S, Abbas S. Lung Cancer: Risk Factors, Management, And Prognosis. IOSR Journal of Dental and Medical Sciences (IOSR-JDMS). 2016;15: 94-101.

3. Kenfield SA, Wei EK, Stampfer MJ, Rosner BA, Colditz GA. Comparison of aspects of smoking among the four histological types of lung cancer. Tobacco control. 2008;17: 198-204.

4. Rosti G, Bevilacqua G, Bidoli P, Portalone L, Santo A, Genestreti G. Small cell lung cancer. Annals of Oncology. 2006;17 Suppl 2: ii5-10.

5. Rennebeck G, Martelli M, Kyprianou N. Anoikis and survival connections in the tumor microenvironment: is there a role in prostate cancer metastasis? Cancer research. 2005;65: 11230-11235.

6. Gilmore AP. Anoikis. Cell Death and Differentiation. 2005;12 Suppl 2: 1473-1477.

7. Buchheit CL, Weigel KJ, Schafer ZT. Cancer cell survival during detachment from the ECM: multiple barriers to tumour progression. Nature Reviews: Cancer. 2014;14: 632-641.

8. Frisch SM, Screaton RA. Anoikis mechanisms. Current Opinion in Cell Biology. 2001;13: 555-562.

9. Paoli P, Giannoni E, Chiarugi P. Anoikis molecular pathways and its role in cancer

progression. Biochimica et Biophysica Acta (BBA) - Bioenergetics. 2013;1833: 3481-3498.

10. Voulgari A, Pintzas A. Epithelial-mesenchymal transition in cancer metastasis: mechanisms, markers and strategies to overcome drug resistance in the clinic. Biochimica et Biophysica Acta (BBA) - Bioenergetics. 2009;1796: 75-90.

11. Coloff JL, Brugge JS. Coping with the metabolic stress of leaving home. Cell Research. 2016;26: 757-758.

12. Davidson SM, Papagiannakopoulos T, Olenchock BA, et al. Environment impacts the metabolic dependencies of Ras-driven non-small cell lung cancer. Cell metabolism. 2016;23: 517-528.

13. Wahl SA, Dauner M, Wiechert W. New tools for mass isotopomer data evaluation in 13C flux analysis: mass isotope correction, data consistency checking, and precursor relationships. Biotechnology and Bioengineering. 2004;85: 259-268.

14. Wiechert W, Mollney M, Petersen S, de Graaf AA. A universal framework for 13C metabolic flux analysis. Metabolic Engineering. 2001;3: 265-283.

15. Duckwall CS, Murphy TA, Young JD. Mapping cancer cell metabolism with13C flux analysis: Recent progress and future challenges. Journal of carcinogenesis. 2013;12.

16. Lane AN, Fan TW. NMR-based Stable Isotope Resolved Metabolomics in systems biochemistry. Archives of Biochemistry and Biophysics. 2017;628: 123-131.

17. Fan TW, Lane AN, Higashi RM, et al. Altered regulation of metabolic pathways in human lung cancer discerned by 13 C stable isotope-resolved metabolomics

(SIRM). Molecular Cancer. 2009;8: 41.

18. Sellers K, Fox MP, Bousamra M, 2nd, et al. Pyruvate carboxylase is critical for non-small-cell lung cancer proliferation. Journal of Clinical Investigation. 2015;125: 687-698.

19. Marin-Valencia I, Cho SK, Rakheja D, et al. Glucose metabolism via the pentose phosphate pathway, glycolysis and Krebs cycle in an orthotopic mouse model of human brain tumors. NMR in Biomedicine. 2012;25: 1177-1186.

20. Jitrapakdee S, St Maurice M, Rayment I, Cleland WW, Wallace JC, Attwood PV. Structure, mechanism and regulation of pyruvate carboxylase. Biochemical Journal. 2008;413: 369-387.

21. Jeoung NH, Harris CR, Harris RA. Regulation of pyruvate metabolism in metabolic-related diseases. Reviews in Endocrine and Metabolic Disorders. 2014;15: 99-110.

22. Jitrapakdee S, Nezic MG, Cassady AI, Khew-Goodall Y, Wallace JC. Molecular cloning and domain structure of chicken pyruvate carboxylase. Biochemical and Biophysical Research Communications. 2002;295: 387-393.

23. Kamarajugadda S, Stemboroski L, Cai Q, et al. Glucose oxidation modulates anoikis and tumor metastasis. Molecular and Cellular Biology. 2012;32: 1893-1907.

24. Hanukoglu I, Rapoport R. Routes and regulation of NADPH production in steroidogenic mitochondria. Endocrine research. 1995;21: 231-241.

25. Rush GF, Gorski JR, Ripple MG, Sowinski J, Bugelski P, Hewitt WR. Organic hydroperoxide-induced lipid peroxidation and cell death in isolated hepatocytes.

Toxicology and Applied Pharmacology. 1985;78: 473-483.

26. Kim H, Sung JY, Park EK, et al. Regulation of anoikis resistance by NADPH oxidase 4 and epidermal growth factor receptor. British Journal of Cancer. 2017;116: 370-381.

27. Chiarugi P, Giannoni E. Anoikis: a necessary death program for anchorage-dependent cells. Biochemical Pharmacology. 2008;76: 1352-1364.

28. Taddei ML, Giannoni E, Fiaschi T, Chiarugi P. Anoikis: an emerging hallmark in health and diseases. Journal of Pathology. 2012;226: 380-393.

29. Kim Y-N, Koo KH, Sung JY, Yun U-J, Kim H. Anoikis resistance: an essential prerequisite for tumor metastasis. International journal of cell biology. 2012;2012.

국문초록

아노이키스(Anoikis) 환경에서 폐 정상세포와 폐암 세포의 대사양상비교

추 문 기

서울대학교 약학대학원

약학과 천연물과학전공

폐암은 암이 진행되기 전까지 증세가 거의 없어 조기발견이 어렵고 생존율이 낮은 치명적인 질병이다. 또한 폐암의 2015 년 사망률은 전체 암 사망자 중 22.6%으로 암으로 인한 사망률 중 가장 높다. 암은 전이(metastasis)가 일어나지 않는다면 원래 발생한 부위에서 외과적으로 완전히 제거될 수 있다. 일반적으로 정상세포는 기질과의 상호작용이 없어지면 생체의 방어기작으로서 아노이키스를 일으켜 죽게 되는 반면

암세포는 생존할 수 있고 이것이 암 전이의 초기 과정에서 중요한 역할을 한다. 따라서 암세포가 갖는 아노이키스 저항성에 대하여 연구한다면 암의 전이를 막아 기존의 암 치료법을 발전시킬 수 있을 것이라 여겨진다. 본 연구에서는 정상 세포와 암세포에 대해 아노이키스 환경에서의 대사를 비교·분석하여 암세포가 어떻게 아노이키스에 대해 저항성을 가지는지를 대사적측면에서 연구하였다. 우선 아노이키스 환경에서 폐암 세포(A549)와 폐 정상세포(MRC5)의 세포 생존율(cell viability)를 비교하여, 세포생존률의 차이가 나기 시작하는 시점인 8 시간, 가장 많이 차이 나는 29 시간으로 시간 조건을 확립하였다. 두 시간대에서 대사체학적 분석을 적용한 결과, MRC5 에서 아노이키스 환경에 노출된 시간이 길수록 GSH(reduced)/total glutathione 의 비율이 낮아짐을 확인하였고, 이는 정상 세포인 MRC5 가 산화적 스트레스 (oxidative stress)가 증가된 것을 극복하지 못해 죽는다는 것을 알 수 있다. 또한 에너지 대사체(ATP,CTP 등)는 stable isotope labeling 을 이용한 13C glucose flux 데이터에서 MRC5 의 경우 아노이키스 환경 29 시간에서 M+5 가 특히 많이 감소한 것을 볼 수 있었다. 이는 glucose 가 ATP 로 만들어지는 과정 중 PPP(pentose phosphate pathway) 후 퓨린·피리미딘 합성을 거치게 되는데, 그 중 퓨린·피리미딘 합성 과정 중 PPAT 가 감소하기 때문인 것이라 생각되었으며 이를 real-time PCR 을 통해 확인할 수 있었다. 암세포의 측면에서는 A549 의 PC(pyruvate carboxylase)가

아노이키스 조건 8 시간 대비 29 시간에서 뚜렷하게 증가하였음을 확인하였다. 또한 NADPH 의 총량이 A549 에서 많았고, 이는 PPP(pentose phosphate pathway)를 활발히 이용하고 있으며 결과적으로 아노이키스 조건에서 암세포의 생존에 기여할 것으로 생각되었다. 위와 같이 정상세포와 암세포에서 아노이키스 저항성 mechanism 에 대사적차이가 중요한 역할을 할 것이며 이는 앞으로 폐암에 대한 전이 및 저항성 연구에 새로운 시각을 제공할 수 있을 것이라 생각된다.

주요어: 아노이키스(anoikis), 아노이키스 저항성(anoikis resistance), 폐암(lung cancer), 전이(metastasis), 대사체학(metabolomics)

학번: 2016-21857